Limnol. Oceanogr., 50(5), 2005, 1352–1361

The effect of ultraviolet radiation on freshwater planktonic primary production: The role of recovery and mixing processes

Véronique P. Hiriart-Baer[1] *and Ralph E. H. Smith*
Department of Biology, University of Waterloo, Waterloo, Ontario N2L 3G1, Canada

Abstract

We used a spectrally resolved kinetic model to calculate ultraviolet radiation (UVR) and photosynthetic active radiation (PAR)-dependent photoinhibitory losses in planktonic primary production in a large lake (Lake Erie) under mixing and water transparency scenarios typical of current and possible future environmental conditions. The model, previously calibrated for Lake Erie phytoplankton, also provided estimates of photoinhibition recovery rates under high irradiance conditions that were compared against direct measurements of recovery rates under lower irradiance. Extensive recovery of photosynthesis, even after severe (80%) inhibition, occurred after transfer to benign, low irradiance conditions. Measured recovery rate constants were independent of preexposure treatment (median of 1.70×10^{-4} s^{-1}) and were comparable to modeled rates under higher radiation fluxes (2.10×10^{-4} s^{-1}). Recovery rates were sufficient to allow near-full recovery within one photoperiod, even after severe inhibition (<6 h). Estimates of the photoinhibitory loss of primary production, integrated through the mixed layer, were not greatly affected by mixing rate variations but were higher in all scenarios with finite mixing rates than in those with no mixing. Modeled 20% stratospheric ozone reductions resulted in small increases in integrated UVR photoinhibition (<1%), as did 20% and 50% changes in dissolved organic carbon (DOC) concentration, whereas increased maximum water clarity scenarios decreased integrated photoinhibition estimates. While UVA, not UVB or PAR, caused most of the photoinhibition in Lake Erie phytoplankton, the extent of integrated photoinhibition is likely to depend mostly on algal physiological parameters of UVR susceptibility (sensitivity and recovery) and the ratio of mixing depth to PAR and UVR photic depths.

The main targets of ultraviolet radiation (UVR) in phytoplankton are DNA and photosystem II structural proteins (D1), so recovery from exposure likely involves both the repair of damaged DNA and the de novo synthesis of chloroplast proteins. Some of the enzymes involved in repairing damaged DNA are inducible. The transcription of photolyase is under light control and is inducible by UVB in plants, and DNA polymerase and DNA ligase are also inducible (Pang and Hays 1991; Greenberg et al. 1997). The control of transcription of these different enzymes is under regulatory control by kinases that are involved in signal transduction and are themselves inducible by growth arrest and DNA damage (Pang and Hays 1991). Evidence for the necessity of de novo chloroplast protein synthesis for recovery of photosynthetic activity comes from experiments, specifically those that use streptomycin to inhibit chloroplast protein synthesis (Lesser et al. 1994; Ihle 1997). In the presence of this protein synthesis inhibitor, recovery does not occur.

Recovery of photosynthesis and related processes from UVR-dependent photoinhibition may require only few hours or >20 h (e.g., Larkum and Wood 1993; Hermann et al. 1997). The variation is likely due to differences in endpoint measurements (e.g., DNA photoproduct removal, oxygen evolution, quantum yield, photosynthesis), length and spectral quality of exposure conditions, and algal taxa used by different investigators (Karentz et al. 1991; Schofield et al. 1995; Hazzard et al. 1997). For example, full recovery of optimal quantum yield (measured as F_v/F_m) and O_2 evolution in *Dunaliella salina* was achieved after short exposures (30 min) to natural solar radiation, but recovery was still incomplete after 21 h when the exposure was 3 h in duration and included mainly UVB (280–320 nm) and short UVA (320–400 nm) radiation (Hermann et al. 1997). The wavelength dependence of recovery was also observed in a macroalga, *Palmaria palmata*, for which exposure to progressively shorter wavelengths increased the degree of photoinhibition and delayed the onset of recovery in the field (natural photoperiod) (Hanelt et al. 1997).

Quantifying the impacts of UVR in nature demands knowledge of recovery as well as damage rates and is further complicated by the difficulty of measuring or modeling the spectral exposure regime in the natural environment (Buma et al. 1996). Mixing in aquatic systems transports phytoplankton through strong vertical gradients of spectral quality and quantity of radiation, and the resulting degree of photoinhibition depends on the strength (i.e., rates) and depth of mixing (Franks and Marra 1994) as well as the spectral transmission properties of the water column. Relatively few studies have attempted to quantify the effects of mixing on the vertically integrated (i.e., areal) rate of primary production, but two kinds of approaches have been taken. The first involves physical simulations of the effects of mixing (e.g., Helbling et al. 1994; Zagarese et al. 1998; Köhler et al. 2001). The second approach employs models that use quan-

[1] To whom correspondence should be addressed. Present address: Environmental Monitoring and Reporting Branch, Ontario Ministry of the Environment, 125 Resources Road, Etobicoke, Ontario M9P 3V6, Canada (veronique.hiriartbaer@ene.gov.on.ca).

Acknowledgments

We would like to thank Patrick Neale and one anonymous reviewer for helping to improve the manuscript. We thank Technical Operations and the officers and crew of the CCGS *Limnos*, who provided valuable assistance in the field. This research was supported by National Sciences and Engineering Research Council and Environment Canada grants to R.S.

titative functions to describe the spectral and time dependence of biological responses (biological weighting functions [BWFs]), together with additional functions, to simulate the mixing and optical regime in the water column (e.g., Franks and Marra 1994; Neale et al. 1998*b*). The influence of mixing on the extent of photoinhibition has been related to the sensitivity of the organisms to UVR (Neale et al. 1998*b*; Zagarese et al. 1998; Boelen et al. 2000) and to the kinetics of photoadaptation with respect to the mixing and optical characteristics of the water column (Cullen and Lewis 1988; Franks and Marra 1994). Vertical mixing will invariably cause different phytoplankton cells within the same water column to possess various histories with respect to light exposure, so knowledge of the appropriate BWFs, including the kinetics of UVR-associated damage and recovery, is critical (Cullen and Lesser 1991; Lesser et al. 1994; Neale et al. 1998*b*).

In a previous article (Hiriart-Baer and Smith 2004), we introduced a new spectrally resolved kinetic model for UVR-dependent photoinhibition of Lake Erie phytoplankton and presented measurements of recovery rates and BWFs for the photoinhibition of primary production. This article begins by evaluating rates of recovery under relatively high (and damaging) irradiance, as predicted by the model, in comparison to experimentally measured recovery rates under lower (nondamaging) irradiance. Using relationships previously defined for Lake Erie between UVR attenuation and more frequently measured limnological variables (Smith et al. 1999), the characteristic spectral irradiance attenuation for each of the lake's three main basins was then defined. The photoinhibition model was then combined with an incident radiation spectrum representative of early summer (high UVR) conditions to calculate the impact of present-day and possible future levels of UVR on primary production. The purpose was not to obtain definitive estimates of the actual degree of photoinhibitory losses, which would require more data on biological response factors and in situ spectral irradiance than were available, but to compare the influence of some of the factors (notably mixing processes and incident radiation spectra) commonly considered important to UV-dependent photoinhibition. The results indicated that variations in the physiological attributes of the phytoplankton (sensitivity to damage and rates of recovery) and penetration of UVA, within the known range of variation in Lake Erie, are much more important to photoinhibition than are variations in mixing rates or ozone-related changes in the incident radiation spectrum. Alterations in spectral transparency and mixing depths associated with climate changes and anthropogenic influences have a large potential to influence photoinhibition of lake phytoplankton.

Materials and methods

Model for photoinhibition and recovery—In the presence of inhibiting radiation, photosynthesis will be a function of both damage and repair kinetics:

$$\frac{dP_{(t)}}{dt} = -k_1 E^*_{\text{inh}} P(t) + k_2[1 - P_{(t)}] \tag{1}$$

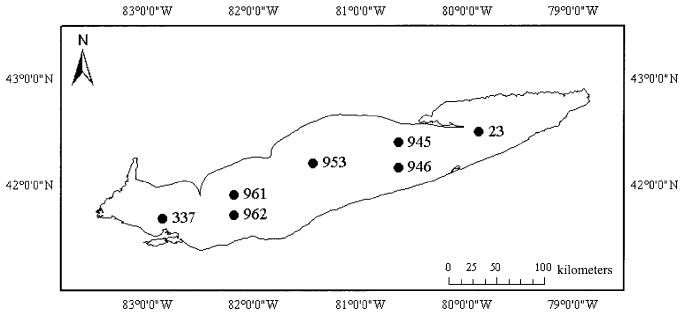

Fig. 1. Map of the sites sampled on Lake Erie in 1997 and 1998.

where $P_{(t)}$ is the photosynthetic rate normalized to an optimal rate (P/P_{opt}) at time t, k_1 and k_2 are the damage and recovery rate constants, respectively; and E^*_{inh} is the biologically weighted inhibitory irradiance (for more details about the model, *see* Hiriart-Baer and Smith 2004). The kinetic model for damage and recovery (''R-model,'' Eq. 1) was fitted to time-course observations of Lake Erie phytoplankton in 1998 under photoinhibiting conditions (Hiriart-Baer and Smith 2004) to provide estimates of damage (k_1, E^*_{inh}) and recovery (k_2) coefficients. If cells are removed from the presence of any inhibiting radiation, photosynthesis is expected to recover with first-order kinetics:

$$\frac{dP'_{(t)}}{dt} = k_2[1 - P'_{(t)}] \tag{2a}$$

and, if integrated over time, this equation becomes:

$$\frac{P_{\text{avg}}}{P_{\text{opt}}} = 1 - \frac{1 - P_{(0)}}{k_2 t}(1 - e^{-k_2 t}) \tag{2b}$$

where t is time since transfer to noninhibiting recovery conditions ($t = 0$ at the beginning of the recovery phase), P_{avg} is the average photosynthetic rate from the beginning of the recovery exposure to time t, and $P_{(0)}$ is the average photosynthetic rate at the beginning of the recovery phase, where both rates are normalized to an optimal rate, P_{opt}. Using Eq. 2b, we can estimate k_2, and once this value is known, we can solve the equation to determine the expected time for recovery to 90% of the optimal photosynthetic rate.

Experimental procedures for recovery rate measurements—The water sampling and experimental protocols for photoinhibition experiments are presented fully elsewhere (Hiriart et al. 2002; Hiriart-Baer and Smith 2004). Briefly, water samples from the epilimnion (5 m) of seven lake stations (Fig. 1) were used to measure the response of primary production rates (^{14}C assimilation into the total organic fraction) to various spectral exposure regimes in temperature-controlled deck boxes. The recovery experiments described here involved a 2-h exposure to damaging radiation treatments (photosynthetic active radiation [PAR] + UVA + UVB or PAR + UVA, at 100% and 50% of surface incident flux), followed by transfer to nondamaging radiation treatments (5% or 10% of surface incident flux). Sample containers were 50-ml quartz glass tubes and were sampled at time zero, 0.5, 1.0, and 2.0 h (damage phase) and 4.0, 6.0,

Table 1. Summary of the limnological variables of the stations sampled for time-series recovery experiments conducted on Lake Erie in the summers of 1997 and 1998.

Date	Station	Basin	Epilimnion depth (m)	Temperature at 5 m (°C)	Chl *a* at 5 m (μg L^{-1})	$K_{d\mathrm{PAR}}$ (m^{-1})	Mean PAR % incident
7 May 97	946	C	22	6.0	1.5	0.43	10.6
3 Jun 97	946	C	22*	8.8	2.5	0.29	15.1
4 Jun 97	337	W	9*	13.2	9.8	1.61	6.9
5 Jun 97	961	C	19*	13.4	1.2	0.83‡	6.3
29 Jul 97	23	E	15	22.0	3.5†	0.24	27.0
30 Jul 97	953	C	12	22.2	1.4	0.32	25.5
31 Jul 97	962	C	11	23.7	2.0	0.36‡	24.8
27 Aug 97	337	W	9*	21.1	15.5	1.16	9.6
16 Jul 98	945	C	10	22.9	4.6	0.33	29.2
11 Aug 98	946	C	17.5	23.6	4.9	0.25	22.6

* Water column was isothermal at the time of sampling.
† Note that in vivo Chl *a* fluorescence was not uniformly distributed with the mixed layer on this date.
‡ Value of $K_{d\mathrm{PAR}}$ derived from the following relationship: $K_{d\text{-PAR}} = -0.026 \times \text{transmission} + 2.258$.

and 8.0 h (recovery phase). In 1998 only, two additional spectral treatments were used (PAR only at 50% and 100% of surface incident flux), and an extra sampling time was included, at 3 h. The stations at which recovery experiments were performed are shown in Table 1. The recovery model (Eq. 2b) was fitted to the measured photosynthetic rates by nonlinear regression to estimate k_2.

Modeling photoinhibition in Lake Erie—The modeling package Stella® (version 5.1.1 for Windows™) was used to determine the degree of photoinhibition predicted by the R-model (Eq. 1) for varying conditions of mixing and spectral transparency of the water column. Although inhibition by UVR can be rapid and extensive in surface waters, UVR photic zones are relatively shallow, and mixing moves algal organisms in and out of these potentially damaging water layers. Our goal was to determine the impact of photoinhibition, particularly the UVR-dependent component, throughout the surface mixed layer as expressed by its effect on the daily integrated (areal) primary production.

The photoinhibition was modeled for an algal community with average Lake Erie photosynthetic parameter values (P^b_m = 4.35 C [Chl a^{-1}] h^{-1}, α^b = 7.67 C Chl a^{-1} E^{-1} m^2) that were derived from 46 light gradient incubations performed in 1997 (11, 21, and 14 in the East, Central, and West basins, respectively) (Smith et al. in press) using the model by Platt et al. (1980). To describe the UVR sensitivity of the phytoplankton, an average BWF measured in Lake Erie in 1998 was applied (Hiriart-Baer and Smith 2004). The BWF comprises an array of 52 coefficients at 2-nm waveband intervals from 295 to 400 nm and, like other coefficients used in this study, is available upon request. Recovery rates and sensitivity to PAR were characterized using the median recovery rate constant (4.28×10^{-4} s^{-1}) and PAR effectiveness (i.e., inhibition) coefficients (2.19×10^{-7} [W $m^{-2}]^{-1}$), also measured in 1998.

A representative, clear-sky, and moderate ozone thickness (314 DU; http://es-ee.tor.ec.gc.ca/e/ozone/document.htm), diurnal radiation spectrum (295–700 nm) was measured at a central basin station with an Oriel Instaspec radiometer (Smith et al. 1999) at 20-min intervals and 0.4-nm bandwidth resolution on 31 July 1997 and was used to drive the primary production calculations. While summer days can be as long as 16 h, the 10-h photoperiod modeled in this study was centered on the maximum UVR photoperiod. Radiation before 0940 h and after 1920 h is unlikely to result in photoinhibition, but photosynthesis will continue. For this reason and because our incident spectrum represents the season and conditions of highest incident irradiance, our calculations should approximate the maximum expected degree of photoinhibition. Average PAR attenuation coefficients measured in 1997 (Hiriart et al. 2002) were 0.26, 0.32, and 0.64 m^{-1} for the Eastern, Central, and West basins, respectively, and were used to calculate PAR at depth for average conditions in each basin. To calculate UVR at depth from the incident spectrum, wavelength-specific attenuation coefficients ($K_{d\lambda}$) were used because attenuations of, and biological responses to, UVR are strongly wavelength-dependent. Direct measurements of $K_{d\lambda}$ are relatively few, so values characteristic of each basin were calculated from an empirical model specific to Lake Erie (Smith et al. 1999). The model predicts K_{d320} from PAR attenuation coefficients and total suspended solids (TSS), for which relatively numerous measurements exist:

$$K_{d320} = 1.378 + 0.218\mathrm{TSS} + 0.804K_{d\mathrm{PAR}} \quad (3a)$$

where TSS is measured in mg L^{-1}, and $K_{d\mathrm{PAR}}$ (m^{-1}) is the diffuse PAR attenuation coefficient. $K_{d\lambda}$ for other wavelengths can then be predicted for Lake Erie from the relationship (from Smith et al. 1999 but with corrected regression coefficients):

$$\ln(K_{d\lambda}/K_{d320}) = 3.52 - 0.011\lambda \quad (3b)$$

The input parameters for the photoinhibition modeling are summarized in Table 2.

Table 2. Summary of input modeling parameters for the different modeling scenarios for the East, Central, and West basins of Lake Erie.

	East	Central	West
Epilimnion depth (m)	16.00	13.00	5.00
Complete mixing depth (m)	27.00	17.80	7.60
TSS (mg L^{-1})	0.95	1.40	4.15
$K_{d\mathrm{PAR}}$ (m^{-1})	0.26	0.32	0.64
K_{d320} (m^{-1})	1.79	1.94	2.80
k_2 ($\times 10^{-4}$ s^{-1})	4.28	4.28	4.28
ε_{R300} [$\times 10^{-4}$ (J m^{-2})$^{-1}$]	1.41	1.41	1.41
$\varepsilon_{\mathrm{PAR}}$ [$\times 10^{-7}$ (W m^{-2})$^{-1}$]	2.19	2.19	2.19
P^b_m (C Chl a^{-1} h^{-1})	4.35	4.35	4.35
α^b (C Chl a^{-1} E^{-1} m^2)	7.67	7.67	7.67

Integrated primary production was calculated assuming: (1) a 10-m epilimnion; (2) an unstratified water column using basin-specific median depths; (3) a stratified water column using basin-specific typical epilimnion depths; and (4) a shallow (2 m) ''temporary'' epilimnion for the West basin only.

An organized water motion (Langmuir circulation) was assumed to be the dominant mixing process, and vertical mixing rates were varied between no motion (i.e., static water column) and cycle rates of 0.5 and 5 h. The shape of the circulation cell was a flattened circular spiral determined using a sinusoidal function with a third harmonic approximating the rectangular shape of a typical Langmuir circulation cell (Denman and Gargett 1983). The distribution of algal organisms within this circulation cell resulted in a distribution of biomass that was not uniform with respect to depth; however, the depth sampling frequency was uniform across mixing scenarios. The time step for calculations was 12 min, and integrated inhibition estimates were modeled for a 10-h photoperiod between 0940 and 1920 h. Four spectral conditions were simulated: (1) PAR + UVA + UVB; (2) PAR + UVA; (3) PAR only; and (4) the optimum predicted from the photosynthetic parameters P_m^b and α^b, i.e., no photoinhibition at all. The first three conditions permitted photoinhibition from each waveband to be calculated and compared to the theoretical optimum (condition 4) to determine their individual contributions to the percent inhibition of integrated primary production (PI_{int}). The calculations used 51 theoretical algal organisms that either remained at one point within the water column for the entire photoperiod or moved vertically at different rates and from different starting depths within a Langmuir circulation cell. BWFs and recovery rate constants were assumed to be constant throughout the day.

Additional modeling was performed for the West basin because it was found to be the most UVR sensitive basin (*see Results*) and likely to show the strongest response to different scenarios. First, to assess the effects of variations of the biological coefficients, we performed a sensitivity analysis under complete mixing conditions (mixing depth of 7.6 m) for four different combinations of low (0.14×10^{-4} s^{-1}) and high (6.54×10^{-4} s^{-1}) recovery rate constants and low (1.08×10^{-4} [W m^{-2}]$^{-1}$) and high (16.1×10^{-4} [W m^{-2}]$^{-1}$) UVR sensitivities (i.e., $\lambda_{R(300)}$). These values are representative of the typical range encountered in 1997 and 1998 (Hiriart-Baer and Smith 2004). Second, the impacts that variations in the incident radiation spectra would have on the organisms were predicted for a 20% reduction in ozone thickness (250 DU; typical minima for the region; http://es-ee.tor.ec.gc.ca/e/ozone/document.htm). The radiation spectrum for 250 DU at 42° latitude and 81° longitude was determined using a radiative transfer model, the Tropospheric Ultraviolet and Visible Radiation Model (Madronich 1993). The unweighted UVB irradiance spectra for 314 and 250 DU are illustrated in Fig. 2. Third, the underwater UV radiation spectra were calculated for a 20% and 50% decrease in dissolved organic carbon (DOC), assuming a 2.6 mg L^{-1} DOC ''normal'' concentration (median measured in Lake Erie in 1997) (Smith et al. 1999). In these cases, the K_{d320} was estimated from the relationship (Smith et al. 1999):

$$\ln K_{d\lambda} = -0.0113\lambda + 4.28\mathrm{DOC}^{0.062} \quad (4)$$

where DOC is measured in mg L^{-1}. The predicted K_{d320} value was then used in Eq. 3b to estimate $K_{d\lambda}$ and calculate the underwater spectra. This additional step was performed to minimize the differences in the spectral shape of the predicted attenuation spectrum. Finally, integrated photoinhibition was calculated for observed minima in TSS, and $K_{d\mathrm{PAR}}$ measured in 1997 in the West basin of Lake Erie using Eq. 3b to calculate the underwater UVR spectra.

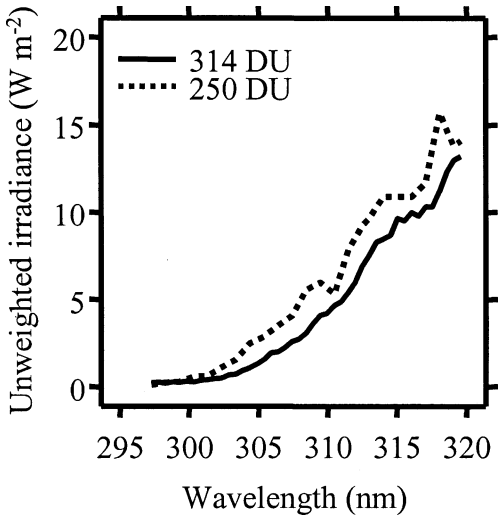

Fig. 2. UVB irradiance spectra under ''normal'' (314 DU) and ''depleted'' (250 DU) stratospheric ozone concentration.

Statistical analysis—Analysis of variance (ANOVA) was used to investigate the dependence of relative cumulative photosynthesis and the measured recovery rates as a function of preexposure treatments. While the k_2 and P'_{final} satisfied the ANOVA assumptions, the $P'_{(0)}$ values were not normally distributed; therefore, these values were logarithm transformed before the ANOVA was performed.

Results

Limnological conditions—Ten recovery experiments were conducted, eight in 1997 and two in 1998. The limnological conditions found at each station sampled on the various dates are listed in Table 1. The conditions observed at all the stations sampled were typical of what has been observed in more extensive samplings relative to temperature, thermal stratification regime, and chlorophyll concentrations.

UVR-dependent inhibition and recovery of photosynthesis—In all experiments, 2 h of exposure resulted in a notable reduction of relative cumulative photosynthesis ($P'_{(t)}$; *see Materials and methods*), and meaningful recovery occurred when the samples were transferred to benign low-light recovery boxes (Fig. 3). The harshest treatment (100% PAR + UVA + UVB) suppressed photosynthesis by ca. 80% in 2 h relative to a light-saturated optimum photosynthetic rate. The mildest treatment (50% PAR only) resulted in lower inhibition, ca. 24% (e.g., Fig. 3b). While UVB additionally suppressed photosynthesis, the bulk of the photoinhibition was due to UVA (Fig. 3). ANOVA showed that $P_{(0)}$ values were significantly (<0.00001) lower in the UVR-exposed (UVA and/or UVB) treatments than in the UVR-shielded treatments within the highest PAR level only (Table 3).

Recovery of relative photosynthetic rates was observed in

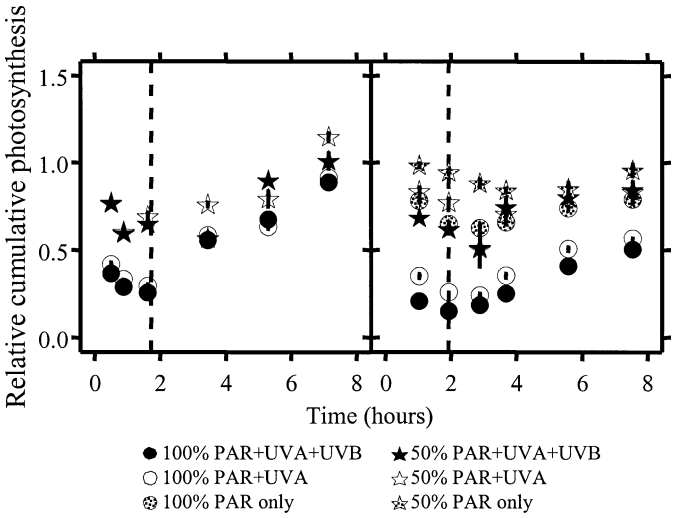

Fig. 3. Temporal changes in relative cumulative photosynthesis for the various 2-h preexposure spectral quality treatments on (left) 31 July 1997 and (right) 11 August 1998. Vertical dashed lines represent the time that samples were transferred to benign recovery deck boxes.

all spectral exposure treatments (Table 3). After 6 h under benign low-light conditions, the harshest treatment (100% PAR + UVA + UVB) had recovered to ca. 64% of the low-light control, and the mildest treatments (100% and 50% PAR only) had recovered to 100% or more. Significant differences in $P'_{(\text{final})}$ values were only observed between the harshest (100S and 100S-) and the mildest (50S- and 50U) treatments (ANOVA; <0.05).

Recovery rate constants and associated recovery times—Recovery rate constants did not differ significantly (>0.8) between exposure treatments (Table 4). In the absence of demonstrable preexposure treatment effects on recovery rate estimates, all treatments were pooled, and an average recovery rate constant was calculated by fitting Eq. 2b for each sample date (Table 5). These recovery rates ranged from 0.46 (4 June 1997) to 8.16×10^{-4} s^{-1} (16 July 1998) and had a median of 1.70×10^{-4} s^{-1} (Table 5). Using an average BWF derived for Lake Erie phytoplankton in 1998 (Hiriart-Baer and Smith 2004), the R-model (Eq. 1) was fit to the corresponding 1997 time-series photosynthesis data (8 h in damage boxes; no corresponding data were available in 1998), and recovery rate constants (k_2) were estimated (Table 5). The range of these values was from 0.30 (e.g., 4 June 1997) to 7.96×10^{-4} s^{-1} (29 July 1997), and the median was 2.10×10^{-4} s^{-1}. ANOVA indicated that the recovery model (Eq. 2b) and R-model (Eq. 1) estimates of k_2 (logarithm transformed) were not significantly different (>0.50). It should be noted that the estimated k_2 rates were likely higher due to the inherent bias of using an average BWF because higher damage rates tend to be associated with higher recovery rates. If actual sensitivity of the algal population sampled in 1997 was lower than that assumed from the average BWF, recovery rates may have been overestimated by the R-model, which may account for the slight discrepancy between measured and estimated rates.

Table 4. Experimentally determined recovery rate constants for the different spectral treatments averaged over all dates ±SE. The values in parentheses are the ranges observed, and the subscripts denote sample size.

Spectral treatment	Recovery rate ($\times 10^{-4}$ s^{-1})
100% PAR + UVA + UVB	$1.42 \pm 0.11_{10}$ (0.25–3.56)
100% PAR + UVA	$1.78 \pm 0.39_{6}$ (0.28–6.39)
100% PAR*	2.17_{1}
50% PAR + UVA + UVB	$2.03 \pm 0.25_{9}$ (0.11–6.92)
50% PAR + UVA	$3.67 \pm 1.03_{6}$ (−0.64–15.94)
50% PAR*	1.2846_{1}

* Only the two 1998 experiments (16 Jul and 11 Aug 98) permitted PAR-only exposure; however, no recovery estimate could be fitted to the data of 16 Jul 98.

Using the median values for recovery rate constants estimated by each method, the time required to achieve 90% recovery of photosynthetic potential was calculated for different degrees of inhibition, assuming that inhibition ceased completely. For severely (80%) inhibited phytoplankton, the recovery times were 5.4 and 3.8 h for the measured and model-estimated recovery rate constants, respectively. For mildly (20%) inhibited phytoplankton, the corresponding times were 1.1 and 0.8 h.

Modeling photoinhibition—Influence of physical processes: Some patterns of spectral composition, transparency, and mixing effects were consistent across all modeling scenarios. (1) PAR-dependent inhibition of integrated primary produc-

Table 3. Relative cumulative photosynthesis for each spectral treatment following 2 h of exposure just before being transferred to the benign recovery deck boxes (initial) and following 6 h of recovery (final). Averages (over all experimental dates) ±1 SE; subscript denotes sample size; values in parentheses represent the range of observed values.

Relative photosynthesis	100% PAR + UVA + UVB	100% PAR + UVA	100% PAR	50% PAR + UVA + UVB	50% PAR + UVA	50% PAR
$P'_{(0)}$	$0.24 \pm 0.02_{11}$ (0.13–0.34)	$0.31 \pm 0.03_{7}$ (0.16–0.44)	$0.58 \pm 0.07_{2}$ (0.50–0.65)	$0.63 \pm 0.05_{11}$ (0.28–0.96)	$0.70 \pm 0.07_{7}$ (0.34–0.94)	$0.76 \pm 0.19_{2}$ (0.57–0.95)
$P'_{(\text{final})}$	$1.06 \pm 0.43_{11}$ (0.36–5.24)	$1.21 \pm 0.50_{7}$ (0.51–4.21)	$0.90 \pm 0.11_{2}$ (0.79–1.01)	$0.95 \pm 0.15_{11}$ (0.65–2.42)	$1.22 \pm 0.29_{7}$ (0.70–2.90)	$1.05 \pm 0.09_{2}$ (0.96–1.13)

Table 5. Recovery model (Eq. 2b) and R-model (Eq. 1) estimates of recovery rate constants for each experimental date. Estimates ± asymptotic standard error of the estimate (or standard error). The r^2 represents the amount of variability explained by the equations used to estimate each recovery rate constant.

	Recovery model		R-model	
Date	k_2 ($\times 10^{-4}$ s^{-1})	r^2	k_2 ($\times 10^{-4}$ s^{-1})	r^2
5 May 97	0.66±0.13	0.946	2.04±1.39	0.502
3 Jun 97	2.11±0.28	0.977	4.01±3.07*	0.562
4 Jun 97	0.46±0.09	0.925	0.30±0.35*	0.583
5 Jun 97	3.30±0.69	0.969	2.15±1.12	0.457
29 Jul 97	0.58±0.06	0.976	7.96±6.26*	0.441
30 Jul 97	1.70±0.18	0.976	1.79±0.76	0.608
31 Jul 97	1.86±0.27	0.973	3.09±1.50	0.498
27 Aug 97	−1.21±0.08	0.876	1.38±0.67	0.490
16 Jul 98	8.16±1.41	0.961	—	—
11 Aug 98	1.26±0.11	0.959	—	—
Median	1.70±0.80	—	2.10±0.83	—

* Recovery rate constant estimate was not significantly different from zero.

tion (PI_{int}) was negligible (<0.1%) in all mixing and transparency scenarios and is therefore not indicated in the tables and figures. (2) PI_{int} predictions for static water column scenarios were always lower than those for mixing (slow or fast) conditions. (3) Vertical mixing rate variations had little effect on PI_{int} (e.g., Fig. 4). (4) UVA-dependent inhibition was always notably higher than UVB-dependent inhibition, even under simulated ozone depletion modeling scenarios (e.g., Fig. 5; Tables 6, 7). (5) A consistent East (lower PI_{int}) to West (higher PI_{int}) gradient in photoinhibition impact was always present (e.g., Fig. 5).

To isolate the effects of water column optical properties on daily PI_{int} estimates, modeling was performed for a hypothetical 10-m water column with optical properties appropriate for each basin (Fig. 4). Under this normalized scenario, estimates of photoinhibition ranged from 4.5% (UVB: 0.6%; UVA: 3.8%, static East basin) to 13.4% (UVB: 1.9%; UVA: 11.5%, mixed West basin). A more realistic assessment of PI_{int} was carried out on a basin-specific basis, simulating different seasonally representative water column dynamics (Fig. 5). Under typical early spring and late fall mixing conditions (i.e., complete mixing conditions; Fig. 5b), estimates of PI_{int} were higher than for typical summer stratified conditions (Fig. 5c), although these differences were small. Total UVR-dependent inhibition ranged from 11.2% to 13.7% and from 10.7% to 12.8% under complete mixing and stratified conditions, respectively, in nonstatic simulations. The differences between the predictions from these mixing scenarios were partially related to the depth of mixing (Z_{mix}) relative to the euphotic depth (Z_{eu}) for each

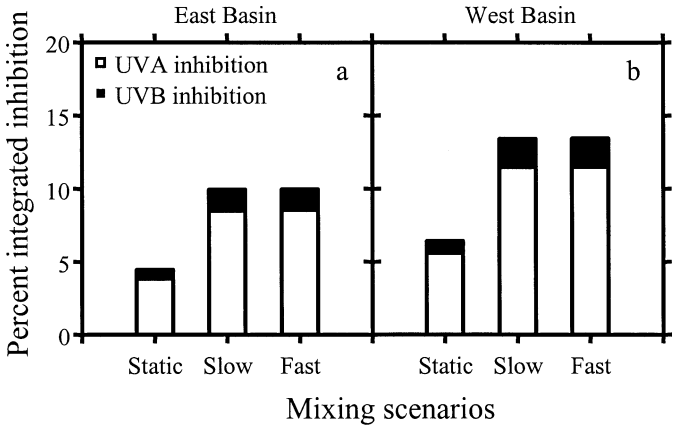

Fig. 4. Inhibition of integrated primary production predictions for typical summer phytoplankton populations mixing down to 10 m in the (a) East and (b) West basins for different water column mixing scenarios.

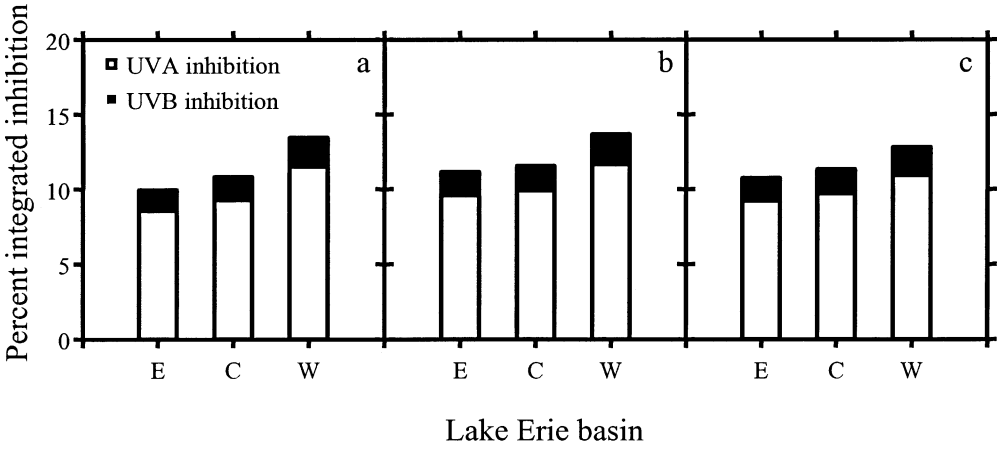

Fig. 5. Basin-specific inhibition of integrated primary production predictions for (a) a 10-m mixed layer, (b) complete mixing, and (c) typical summer epilimnion depths for a water column with a cycle rate of 0.5 h cycle^{-1}. Photosynthesis was integrated to 27, 17.8, and 7.6 m for the E, C, and W basins, respectively, for the complete mixing simulation and to 16, 13, and 5 m for the E, C, and W basins, respectively, for the typical summer epilimnion depth simulations. Although the West basin is commonly uniformly mixed, it does stratify on occasion, and of the stations we sampled, the median epilimnion depth was 5 m.

Table 6. Percent photoinhibition predictions for ''temporary'' thermocline scenarios in the West basin over one photoperiod. A static water column scenario was used for the ''temporary'' thermocline estimates, and these are compared to a complete mixing scenario. *See Table 2* for model parameters used.

	Inhibition		
	UVB	UVA	Total
Top 2 m	1.3	8.8	10.1
Bottom 5.6 m	0.0	0.3	0.3
Integrated water column	0.8	5.4	6.2
Complete mixing (7.6 m)	2.0	11.6	13.6

simulation. As the $Z_{mix}:Z_{eu}$ ratio increased, so did the water column integrated UVR-dependent photoinhibition (Fig. 6).

The potentially damaging effects of shallow ''temporary'' thermoclines were also assessed for the West basin, which has a propensity for developing these ephemeral water column structures under calm conditions (Hiriart et al. 2002). While relative inhibition within the shallow thermoclines can be high (up to 10.1% in our static simulations), when the effects are integrated for the entire water column, PI_{int} estimates are significantly reduced (6.2%) compared to complete mixing (13.6%) conditions (Table 6).

Influence of physiological processes: Given the apparent vulnerability of the West basin to UVR inhibition, a sensitivity analysis was carried out to estimate the range of possible PI_{int} (Fig. 7). These estimates ranged from 0.8% (high recovery and low sensitivity; static) to ca. 44% (low recovery and high sensitivity; mixing) across all water column mixing conditions. At the high end of the range, UVA could inhibit integrated primary production by as much as ca. 40%, while UVB inhibition estimates were ca. 4%. Similar to previous simulations, under these modeled conditions, water column mixing rates had little effect on integrated photoinhibition, and mixing alone increased estimates of PI_{int} under all conditions.

Influence of changing the underwater UVR climate: Continuing to use the West basin as our model basin, we simulated the impacts of a 250-DU ozone, a 20% and 50% decrease in DOC concentration, and a maximum water clarity scenario (Table 7). The reduced ozone scenario increased

Table 7. Percent photoinhibition predictions for the West basin under a complete mixing scenario for different UVR climate data over one photoperiod (0940 to 1920 h). Values are averaged over both slow and fast mixing rate scenarios. *See Table 2* for model parameters used.

	Inhibition		
	UVB	UVA	Total
''Normal'' conditions	2.0	11.6	13.6
250-DU ozone thickness	2.4	11.6	14.0
20% DOC depletion	2.1	12.3	14.4
50% DOC depletion	2.2	12.7	14.9
Minimum TSS and $K_{d\mathrm{PAR}}$	1.6	9.4	11.0

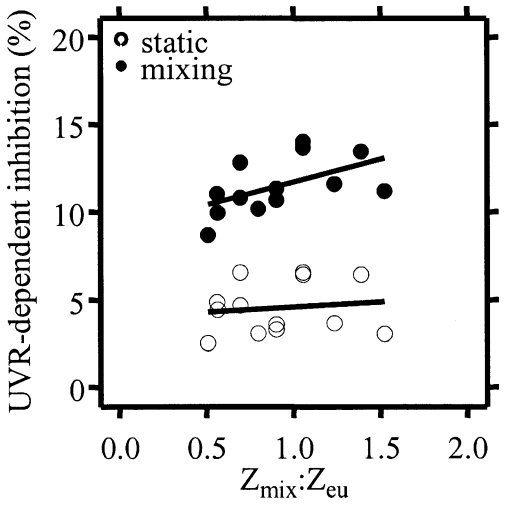

Fig. 6. Relationship between UVR-dependent inhibition and $Z_{mix}:Z_{eu}$ for all Lake Erie basins across all mixing scenarios. The estimates for each Lake Erie basin under a 10-m mixed layer, complete mixing, and typical epilimnion depth as well as the estimates under minimum TSS and $K_{d\mathrm{PAR}}$ for all three basins and the shallow temporary thermocline simulations for the West basin are included. The solid lines are Systat linear smoothers.

PI_{int} estimates by <1% (13.6–14.0%); similarly, the simulated reductions in DOC concentrations caused small (<2%; 13.6–14.9%) increases of PI_{int}. On the other hand, estimates of integrated photoinhibition under a maximum water clarity scenario, i.e., minimum TSS and $K_{d\mathrm{PAR}}$, were lower (13.6–

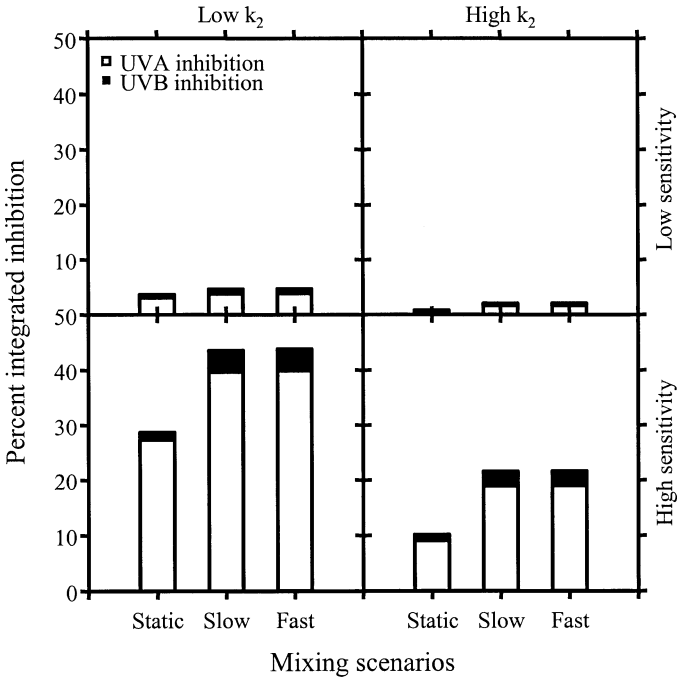

Fig. 7. Sensitivity analysis of integrated photoinhibition predictions using two levels of recovery rate constants and overall UVR sensitivity under different mixing scenarios. Low and high k_2 values: 0.14 and 6.54 $\times$ 10^{-4} s^{-1}. Low and high sensitivity: $\lambda_{R(300)}$: 1.08 and 16.1 $\times$ 10^{-4} ($[J\ m^{-2}]^{-1}$).

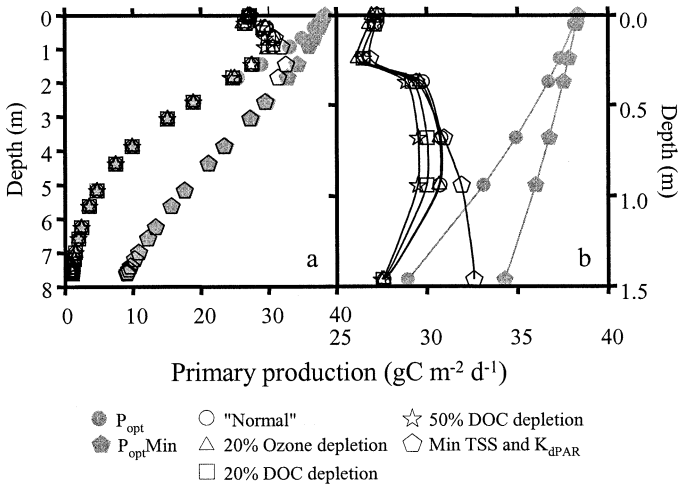

Fig. 8. Vertical profiles of primary production in Lake Erie phytoplankton under different incident radiation spectra and underwater transparency scenarios. Note the difference in depth between panels a and b. P_{opt}MIN defines the optimum vertical profile of primary production under minimum TSS and K_{dPAR} conditions.

11%). The lower relative photoinhibition of integrated primary production under this latter scenario is related to the increase in uninhibited primary production at depth as a function of increased water clarity (Fig. 8).

Discussion

The susceptibility of photosynthesis to damage by UVR is composed of at least two important and distinct components: (1) a component that involves a sensitivity to damage and is partly influenced by the presence of photoprotective pigments (e.g., Schofield et al. 1995) and (2) a component that involves the ability to recover and is mediated by repair processes (e.g., Karentz 1999). The first component of UVR susceptibility has been studied by numerous researchers who were mostly investigating the presence and/or induction of mycosporine-like amino acids, a category of pigments typically associated with UVR photoprotection in microalgae (e.g., Roy 2000). The second component of UVR susceptibility, the ability to photorecover, has received comparatively little attention despite its obvious importance in the integrated response of primary producers to damaging UVR.

It can be argued that inhibition by UVR can either be reduced or increased within a mixed water column compared to a static one. On an individual basis, production of one algal organism may likely be favored when the water column is in motion, since mixing will inevitably provide shelter from damaging UVR. On the other hand, from an integrative point of view, considering the entire water column, mixing has the disadvantage of exposing more of the algal biomass to high-light, photoinhibiting, surface waters (Neale et al. 1998*b*). In this study, Lake Erie phytoplankton demonstrated meaningful recovery of photosynthesis after 2 h of exposure to damaging radiation. Our estimates of recovery rates would allow, under mild inhibiting conditions (20%), near-full recovery of photosynthesis (time to 90% recovery; 0.8–1.1 h) within a summer photoperiod (on average, from 0600 to 2000 h for the 42° latitude between 21 June and 21 September). In the absence of carry over from one day to the next, we can focus our efforts on modeling inhibition for one photoperiod and evaluate the effects of physiological, physical, and optical parameters on the photoinhibition of integrated primary production.

From a physiological perspective, the sensitivity and recovery potential of algal photosynthesis significantly affected our PI_{int} estimates. The range in UVR sensitivity found in Lake Erie was large enough to elicit up to a 10-fold difference in predicted integrated inhibition impacts in a mixed water column. Although the mitigating effects of recovery rates appeared to be less important than the inhibiting effects of sensitivity (2- vs. 10-fold differences; Fig. 7), recovery processes are nevertheless essential for photosynthetic recovery within the day, because they prevent an accumulation of inhibition over successive days. During our typical parameter simulations (Table 2), inhibition of relative photosynthesis in the West basin could reach ca. 32% during the day, yet active recovery resulted in near-maximum rates of photosynthesis (0.96 relative photosynthesis) being reached at the end of our simulations.

From a physical perspective, we found that mixing alone increased our estimates of inhibition. This follows a number of studies that have assessed the effects of mixing on UVR-dependent inhibition (e.g., Helbling et al. 1992). This effect is related to the nonlinear response of photoinhibition over time, specifically the rapid onset of UVR-dependent photoinhibition (e.g., Hiriart et al. 2002; Neale et al. 2003). Under static conditions, decreases in relative photosynthesis are small after the first few hours of exposure as a steady state is reached, while under mixing conditions large decreases in production are continuously being observed as new uninhibited phytoplankton are exposed to high surface UVR irradiances (Neale et al. 2003). The rate of vertical mixing and the depth of mixing may also influence the extent of UVR-dependent inhibition, although the relationship is not straightforward (Neale et al. 1998*b*). Antarctic phytoplankton mixing to depths well below the euphotic zone have shown reduced integrated water column inhibition compared to communities that mix within the euphotic zone (Neale et al. 1998*b*). Furthermore, in shallow (≤42 m) mixed layers, slow mixing (e.g., 1-h cycle time) lessened inhibition predictions for this polar algal community compared to fast mixing (20-min cycle time). We observed only small differences (<0.1%) between mixing rates, with higher estimates of PI_{int} under fast mixing (0.5-h cycle) conditions compared to slow (5-h cycle) mixing rates. These patterns of results are similar to those observed by Huot et al. (2000) in marine bacterioplankton, DNA dimer accumulation. The authors observed no differences in integrated inhibition estimates under various mixing rates (measured as wind speed), but the distribution of that inhibition was related to mixing rates. Perhaps the range of depth, water clarity, and algal physiological parameters limited our scope for detecting differences in photoinhibition under various mixing depth and mixing rate simulations. Furthermore, the Antarctic study applied a different kinetic model, one that assumed no repair capabilities and predicted photosynthesis as a function of cumulative exposure to inhibiting radiation (Neale et al. 1998*a*; Hir-

iart-Baer and Smith 2004). Inhibited rates of photosynthesis predicted by this model would be maintained throughout the mixing simulation, while the R-kinetic model used in this study would permit some recovery at depth, which would help minimize the effects of mixing rate. In fact, when we assumed no active recovery for a completely mixed West basin (7.6 m Z_{mix}), slower mixing rates enhanced PI_{int} by ca. 5% compared to ca. 0.3% under typical recovery rate conditions.

The extent of recovery at depth will depend on the time spent below the euphotic depth, where adequate light for uninhibited primary production and photoenzymatic repair is unavailable. This dependence was reflected in the relationship between predicted UVR-dependent inhibition and the $Z_{mix}:Z_{eu}$ ratio. Integrated photoinhibition of primary production for algal organisms mixed below the euphotic zone was higher than for those remaining above the euphotic depth. Our results differ from those presented by Barbieri et al. (2002); however, we did not consider the seasonal variability of algal physiological parameters that would accompany the seasonal changes of $Z_{mix}:Z_{eu}$, so a direct comparison with these results is difficult. Further and more specific modeling that incorporates seasonally variable k_2, P^b_{max}, and α^b would be needed for a direct comparison to the Barbieri et al. (2002) study.

From an optical perspective, it is evident how water column optical characteristics are critical determinants for UVR exposure and, by extension, photoinhibition. Globally, light attenuation will depend on light scattering and light absorption by water itself, dissolved organic matter, and particulate organic matter (e.g., phytoplankton) as well as inorganic matter (Kirk 1994). Specific to UVR, dissolved organic matter seems to be particularly influential (Scully and Lean 1994), although TSS can also be important (Smith et al. 1999). Lake Erie is spatially heterogeneous in its transmission properties, typically demonstrating high water clarity in the East basin and lower water clarity in the West basin (Smith et al. 1999). Relative daily PI_{int} estimates were higher in the more turbid West basin than in the clearer East and Central basins. While counterintuitive, this is a direct consequence of differences in available refuges from photoinhibiting radiation. Given basin specific typical euphotic depths, the East, Central, and West basins have 24%, 28%, and 39% of their euphotic zone occupied by their UVR-photic zone, respectively. This allows more unabated primary production to occur in the East versus West basin photic zones, resulting in lower relative estimates of integrated photoinhibition in the East compared to the West basin.

Constant across all simulations was the relatively minor PAR and UVB-dependent inhibition and the significant UVA-dependent inhibition. While UVA can be beneficial to phytoplankton by inducing, for example, photoenzymatic repair processes (Mitchell and Karentz 1993; Roy 2000), it can also severely inhibit primary production (Bühlmann et al. 1987; Helbling et al. 1992; Neale et al. 1994). UVA has a much lower photoinhibition efficiency than UVB because of its lower energetic content (Ghetti et al. 1998); however, the flux of incident UVA is ca. 10-fold higher than that of UVB, inevitably resulting in more UVA-dependent inhibition in the natural environment. The overall importance of UVA in photoinhibition was also true for our most severe case, i.e., complete mixing 250-DU ozone simulation, where UVB-dependent inhibition was responsible for ca. 3% compared to ca. 11% UVA-dependent inhibition.

Similar to the DNA dimer accumulation study by Huot et al. (2000), this study found relatively large changes in DOC had little effect on the estimates of integrated primary production (Table 7). While increases in DOC may reduce UVR exposure, this also reduces productivity at depth so that, integrated over the entire water column, changes in DOC concentrations counteract each other (Huot et al. 2000). Furthermore, while DOC strongly absorbs in the UVA part of the spectrum, the relationship between DOC and K_{d320} at a concentration of about 2.6 mg L^{-1} is relatively flat and results in only a 20% change in K_{d320}. This small effect on K_{d320} was reflected in the relatively small change in photoinhibition predicted from the 50% change in DOC. Under static water column scenarios (Fig. 8), it is clear that while changes in the underwater UVR climate can lead to differences in the shallow waters (<2 m), the effects of increased UVR penetration are quickly muted by rapid absorption of these wavelengths, which leads to small increases in PI_{int} over the entire water column.

In conclusion, it appears that physiological parameters (sensitivity and recovery potential) and the depth of mixing relative to the euphotic (and UVR) depth are the most important factors influencing inhibition of integrated primary production. While the transparency of aquatic systems to UVR is an important determinant of photoinhibition, it must be put into context with respect to overall UVR exposure, which is inherently dependent on physical forces (mixing depth) and physical boundaries (basin depth). Shallow aquatic systems or basins within lakes (e.g., West basin of Lake Erie) that already afford few UVR refuges are likely to be the most at risk.

References

BARBIERI, E. S., V. E. VILLAFAÑE, AND E. W. HELBLING. 2002. Experimental assessment of UV effects on temperate marine phytoplankton when exposed to variable radiation regimes. Limnol. Oceanogr. **47:** 1648–1655.

BOELEN, P., M. K. DE BOER, G. W. KRAAY, M. J. W. VELDHUIS, AND A. G. J. BUMA. 2000. UVBR-induced DNA damage in natural marine picoplankton assemblages in the tropical Atlantic Ocean. Mar. Ecol. Prog. Ser. **193:** 1–9.

BÜHLMANN, B., P. BOSSARD, AND U. UEHLINGER. 1987. The influence of longwave ultraviolet radiation (u.v.-A) on the photosynthetic activity (14C-assimilation) of phytoplankton. J. Plankton Res. **9:** 935–943.

BUMA, A. G. J., H. J. ZEMMELINK, K. SJOLLEMA, AND W. W. C. GIESKES. 1996. UVB radiation modifies protein and photosynthetic pigment content, volume and ultrastructure of marine diatoms. Mar. Ecol. Prog. Ser. **143:** 47–54.

CULLEN, J. J., AND M. P. LESSER. 1991. Inhibition of photosynthesis by ultraviolet radiation as a function of dose and dosage rate: Results for a marine diatom. Mar. Biol. **111:** 183–190.

———, AND M. R. LEWIS. 1988. The kinetics of algal photoadaptation in the context of vertical mixing. J. Plankton Res. **10:** 1039–1063.

DENMAN, K. L., AND A. E. GARGETT. 1983. Time and space scales

of vertical mixing and advection of phytoplankton in the upper ocean. Limnol. Oceanogr. **28:** 801–815.

FRANKS, P. J. S., AND J. MARRA. 1994. A simple new formulation for phytoplankton photoresponse and an application in a wind-driven mixed layer model. Mar. Ecol. Prog. Ser. **111:** 143–153.

GHETTI, F., S. FUOCO, AND G. CHECCUCCI. 1998. UVB monochromatic action spectrum for the inhibition of photosynthetic oxygen production in the green alga *Dunaliella salina.* Phytochem. Photobiol. **68:** 276–280.

GREENBERG, B. M., M. I. WILSON, X.-D. HUANG, C. L. DUXBURY, K. E. GERHARDT, AND R. W. GENSEMER. 1997. The effects of ultraviolet-B radiation on higher plants, p. 1–35. *In* W. Wang, J. W. Gorsuch, and J. S. Hughes [eds.], Plants for environmental studies. CRC Press LLC.

HANELT, D., C. WIENCKE, AND W. NULTSCH. 1997. Influence of UV radiation on the photosynthesis of Arctic macroalgae in the field. J. Photochem. Photobiol. B Biol. **38:** 40–47.

HAZZARD, C., M. P. LESSER, AND R. A. KINZIE III. 1997. Effects of ultraviolet radiation on photosynthesis in the subtropical marine diatom, *Chaetoceros gracilis* (Bacillariophyceae). J. Phycol. **33:** 960–969.

HELBLING, E. W., V. VILLAFAÑE, M. FERRARIO, AND O. HOLM-HANSEN. 1992. Impact of natural ultraviolet radiation on rates of photosynthesis and on specific marine phytoplankton species. Mar. Ecol. Prog. Ser. **80:** 89–100.

———, ———, AND O. HOLM-HANSEN. 1994. Effects of ultraviolet radiation on Antarctic marine phytoplankton photosynthesis with particular attention to the influence of mixing, p. 207–227. *In* C. S. Weiler and P. A. Penhale [eds.], Ultraviolet radiation in Antarctica: Measurements and biological effects. Antarctic Research Series. V. 62. American Geophysical Union.

HIRIART, V. P., B. M. GREENBERG, S. J. GUILDFORD, AND R. E. H. SMITH. 2002. Effects of ultraviolet radiation on rates and size distribution of primary production by Lake Erie phytoplankton. Can. J. Fish. Aquat. Sci. **59:** 317–328.

HIRIART-BAER, V. P., AND R. E. H. SMITH. 2004. Models for ultraviolet radiation-dependent photoinhibition of Lake Erie phytoplankton. Limnol. Oceanogr. **49:** 202–214.

HUOT, Y., W. H. JEFFREY, R. F. DAVIS, AND J. J. CULLEN. 2000. Damage to DNA in bacterioplankton: A model of damage by ultraviolet radiation and its repair as influenced by vertical mixing. Photochem. Photobiol. **72:** 62–74.

IHLE, C. 1997. Degradation and release from the thylakoid membrane of Photosystem II subunits after UV-B irradiation of the liverwort *Conocephalum conicum.* Photosynth. Res. **54:** 73–78.

KARENTZ, D. 1999. Evolution and ultraviolet light tolerance in algae. J. Phycol. **35:** 629–630.

———, J. E. CLEAVER, AND D. L. MITCHELL. 1991. Cell survival characteristics and molecular responses of Antarctic phytoplankton to ultraviolet-B radiation. J. Phycol. **27:** 326–341.

KIRK, J. T. O. 1994. Optics of UV-B radiation in natural waters. Arch. Hydrobiol. Beih. Ergebn. Limnol. **43:** 1–16.

KÖHLER, J., M. SCHMITT, H. KRUMBECK, M. KAPFER, E. LITCHMAN, AND P. J. NEALE. 2001. Effects of UV on carbon assimilation of phytoplankton in a mixed water column. Aquat. Sci. **63:** 294–309.

LARKUM, A. W. D., AND W. F. WOOD. 1993. The effect of UV-B radiation on photosynthesis and respiration of phytoplankton, benthic macroalgae and seagrasses. Photosynth. Res. **36:** 17–23.

LESSER, M. P., J. J. CULLEN, AND P. J. NEALE. 1994. Carbon uptake in a marine diatom during acute exposure to ultraviolet B radiation: Relative importance of damage and repair. J. Phycol. **30:** 183–192.

MADRONICH, S. 1993. UV radiation in the natural and perturbed atmosphere, p. 17–69. *In* M. Tevini [ed.], Environmental effects of UV (ultraviolet) radiation. Lewis.

MITCHELL, D. L., AND D. KARENTZ. 1993. The induction and repair of DNA photodamage in the environment, p. 345–377. *In* L. O. Björn, J. Moan, W. Nultsch, and A. R. Young [eds.], Environmental UV photobiology. Plenum Press.

NEALE, P. J., J. J. CULLEN, AND R. F. DAVIS. 1998*a*. Inhibition of marine photosynthesis by ultraviolet radiation: Variable sensitivity of phytoplankton in the Weddell-Scotia Confluence during the austral spring. Limnol. Oceanogr. **43:** 433–448.

———, R. F. DAVIS, AND J. J. CULLEN. 1998*b*. Interactive effects of ozone depletion and vertical mixing on photosynthesis of Antarctic phytoplankton. Nature **392:** 585–589.

———, E. W. HELBLING, AND H. E. ZAGARESE. 2003. Modulation of UV exposure and effects by vertical mixing and advection, p. 107–134. *In* E. W. Helbling and H. E. Zagarese [eds.] UV effects in aquatic organisms and ecosystems. Royal Society of Chemistry.

———, M. P. LESSER, AND J. J. CULLEN. 1994. Effects of ultraviolet radiation on the photosynthesis of phytoplankton in the vicinity of McMurdo Station, Antarctica, p. 125–142. *In* C. S. Weiler and P. A. Penhale [eds.], Ultraviolet radiation in Antarctica: Measurements and biological effects. Antarctic Research Series. V. 62. American Geophysical Union.

PANG, Q., AND J. B. HAYS. 1991. UV-B inducible and temperature-sensitive photoreactivation of cyclobutane pyrimidine dimers in *Arabidopsis thaliana.* Plant Physiol. **95:** 536–543.

PLATT, T., C. L. GALLEGOS, AND W. G. HARRISON. 1980. Photoinhibition of photosynthesis in natural assemblages of marine phytoplankton. J. Mar. Res. **38:** 687–701.

ROY, S. 2000. Strategies for the minimisation of UV-induced damage, p. 177–205. *In* S. J. De Mora, S. Demers, and M. Vernet [eds.], The effects of UV radiation in the marine environment. Cambridge Univ. Press.

SCHOFIELD, O., B. M. A. KROON, AND B. B. PRÉZELIN. 1995. Impact of ultraviolet-B radiation on photosystem II activity and its relationship to the inhibition of carbon fixation rates for Antarctic ice algae communities. J. Phycol. **31:** 703–715.

SCULLY, N. M., AND D. R. S. LEAN. 1994. The attenuation of ultraviolet radiation in temperate lakes. Arch. Hydrobiol. Beih. Ergebn. Limnol. **43:** 135–144.

SMITH, R. E. H., J. A. FURGAL, M. N. CHARLTON, B. M. GREENBERG, V. HIRIART, AND C. MARWOOD. 1999. The attenuation of ultraviolet radiation in a large lake with low dissolved organic matter concentrations. Can. J. Fish. Aquat. Sci. **56:** 1351–1361.

———, V. P. HIRIART-BAER, S. N. HIGGINS, S. J. GUILDFORD, AND M. N. CHARLTON. In press. Planktonic primary production in the offshore waters of dreissenid-infested Lake Erie in 1997. J. Gt. Lakes Res.

ZAGARESE, H. E., B. TARTAROTTI, W. CRAVERO, AND P. GONZALEZ. 1998. UV damage in shallow lakes: The implications of water mixing. J. Plankton Res. **20:** 1423–1433.

Received: 20 August 2004
Accepted: 28 February 2005
Amended: 6 April 2005